Inorg. Chem. **2002**, *41*, 5119–5125

Out-of-Center Distortions in d^0 Transition Metal Oxide Fluoride Anions

Margaret E. Welk, Alexander J. Norquist,[§] Frederick P. Arnold, Charlotte L. Stern, and Kenneth R. Poeppelmeier*

Department of Chemistry, Northwestern University, Evanston, Illinois 60208-3113

Received March 29, 2002

Electronic effects and the bond network are the two factors that cause out-of-center distortions in octahedral d^0 transition metal oxide fluoride anions. Overlap between filled oxide p orbitals and vacant cation d orbitals results in strong, short metal–oxide bonds causing the metal ion to distort toward the oxide ligand. This primary, electronic distortion is not dependent on the extended structure. Smaller, secondary distortions of the anionic octahedra are caused by interactions with the bond network. $[HNC_6H_6OH]_2[Cu(NC_5H_5)_4(NbOF_5)_2]$, prepared with 5-hydroxy-2-methylpyridine that provides two coordination contact sites to the anion when protonated, exhibits distortions in the anion reflecting both factors. Crystal data for $[HNC_6H_6OH]_2[Cu(NC_5H_5)_4(NbOF_5)_2]$: monoclinic, space group *C*2/*c* (No. 15), with $a = 10.9427(8)$ Å, $b = 16.204(1)$ Å, $c = 21.396(2)$ Å, $\beta = 93.263(1)°$, and $Z = 4$. Conditions for detection of both distortion types are discussed with five additional examples.

Introduction

Early transition metal d^0 cations in distorted octahedral environments are key constituents of materials that exhibit important structure-dependent properties such as piezoelectricity, second-order nonlinear optical activity, and ferroelectricity.[1−3] Four factors have been described that contribute to the prevalence of these characteristic out-of-center distortions: electronic effects, bond networks, lattice stresses, and cation−cation repulsions.[4] The first two factors appear to explain the distortions observed in early transition metal oxide fluoride anions of the formula $[MO_xF_{6-x}]^{2-}$ ($x = 1$, M = V, Nb, Ta; and $x = 2$, M = Mo, W). Mixing between vacant cation d orbitals and filled oxide p orbitals, which has been quantified by single point density functional theory (DFT) calculations, results in the formation of strong, short metal−oxide bonds and leads to the "primary" distortion observed in $[MO_xF_{6-x}]^{2-}$ anions. Solid-state bond network interactions within the crystal between the anion and the extended structure cause "secondary" distortions of lesser magnitude. These smaller distortions only modify the intrinsic primary distortion in $[MO_xF_{6-x}]^{2-}$ anions. Comparisons of several structures containing oxide fluoride anions are presented to illustrate the separate and distinct roles that electronic effects and bond network interactions have on out-of-center distortions involving d^0 transition metal cations.

Experimental Section

Caution. $(HF)_x$·pyridine is toxic and corrosive!

Materials. CuO (99.99% Aldrich), Nb_2O_5 (99.99% Aldrich), pyridine (99.8% anhydrous, Aldrich), 5-hydroxy-2-methylpyridine (99% Aldrich), and $(HF)_x$·pyridine (pyridinium poly(hydrogen fluoride), 70 wt % HF, Aldrich) were used as received. Reagent amounts of deionized water were also used in the syntheses.

Synthesis. $[HNC_6H_6OH]_2[Cu(py)_4(NbOF_5)_2]$ (py = NC_5H_5) was synthesized by adding 0.1004 g (3.78×10^{-4} mol) of Nb_2O_5, 0.0600 g (7.55×10^{-4} mol) of CuO, 1.0304 g (9.44×10^{-3} mol) of 5-hydroxy-2-methylpyridine, 0.5999 g (2.28×10^{-3} mol) of $(HF)_x$·pyridine, and 0.0644 g (3.58×10^{-3} mol) of water to a Teflon (fluoro−ethylene−propylene) "pouch".[5] The pouch was sealed and placed into a 2000-mL autoclave (Parr) filled with 600 mL of deionized water. Up to 20 additional pouches with different reactant molar ratios were studied (see Supporting Information). The autoclave was heated to 150 °C for 24 h, and then slow cooled to room temperature over an additional 24 h. The pouches were removed from the autoclave, found to contain no crystalline material, and left unopened. Blue crystals of $[HNC_6H_6OH]_2[Cu(py)_4(NbOF_5)_2]$ were observed after one week. Pouches that contained crystals were opened in air and the crystals were recovered by filtration. The highest yield pouch, approximately 66% yield based on niobium, was described above.

* Author to whom correspondence should be addressed. E-mail: krp@northwestern.edu.

§ Present address: Inorganic Chemistry Laboratory, Oxford University, Oxford, OX1 3QR, U.K.

(1) Hagerman, M. E.; Poeppelmeier, K. R. *Chem. Mater.* **1995**, *7*, 602.
(2) Halasyamani, P. S.; Poeppelmeier, K. R. *Chem. Mater.* **1998**, *10*, 2753.
(3) Jacco, J. C. *SPIE Int. Soc. Opt. Eng.* **1988**, *968*, 93.
(4) Kunz, M.; Brown, I. D. *J. Solid State Chem.* **1995**, *115*, 395.
(5) Harrison, W. T. A.; Nenoff, T. M.; Gier, T. E.; Stucky, G. D. *Inorg. Chem.* **1993**, *32*, 2437.

10.1021/ic025622v CCC: $22.00
Published on Web 09/07/2002

Table 1. Crystallographic Data for $[HNC_6H_6OH]_2[Cu(NC_5H_5)_4(NbOF_5)_2]$

data	$[HNC_6H_6OH]_2[Cu(NC_5H_5)_4(NbOF_5)_2]$
formula	$CuC_{32}H_{36}F_{10}N_6O_4Nb_2$
a (Å)	10.9427(8)
b (Å)	16.204(1)
c (Å)	21.396(2)
β (deg)	93.263(1)
V (Å^3)	3787.6(4)
Z	4
fw	1008.02
space group	$C2/c$ (No. 15)
T (°C)	−120(1)
λ (Å)	0.71069
ρ_{calcd} (g/cm^3)	1.768
ρ_{obsd} (g/cm^3)[a]	1.81(6)
μ (cm^{-1})	12.45
$R(F)$[b]	0.026
$R_w(F)$[c]	0.031

[a] Density measured by flotation pycnometry at 24 °C. [b] $R = \sum||F_o| - |F_c||/\sum|F_o|$. [c] $R_w = [\sum(|F_o| - |F_c|)^2/\sum(F_o)^2]^{1/2}$.

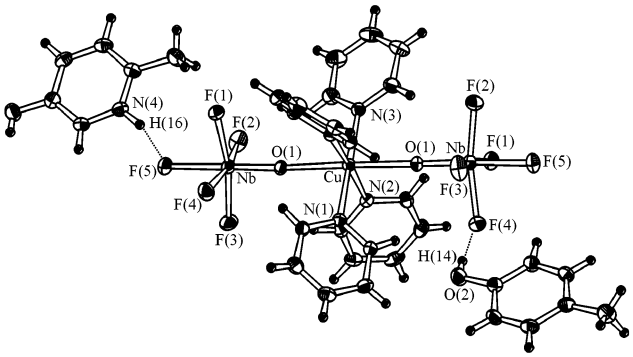

Figure 1. Thermal ellipsoid plot (50% probability) of $[HNC_6H_6OH]_2[Cu(py)_4(NbOF_5)_2]$.

Crystallographic Determination of $[HNC_6H_6OH]_2[Cu(py)_4(NbOF_5)_2]$. All calculations were preformed with the TEXSAN crystallographic software package from Molecular Structure Corp.[6] The structure was solved by direct methods[7] and expanded with Fourier techniques.[8] On the basis of systematic absences and successful solution and refinement of the structure, the space group was determined to be $C2/c$ (No. 15). All atom sites including hydrogen were located from the difference map. Hydrogen atoms were refined by using isotropic thermal parameters. All non-hydrogen atom positions were refined by using anisotropic thermal parameters. See Tables 1 and 2 for relevant crystallographic data and bond lengths, respectively. See Figure 1 for a thermal ellipsoid plot of $[HNC_6H_6OH]_2[Cu(py)_4(NbOF_5)_2]$.

Spectroscopic Measurements. A midinfrared (400−4000 cm^{-1}) spectrum was collected with a Bio-Rad FTS-60 FTIR spectrometer operating at a resolution of 2 cm^{-1}. See Supporting Information.

Computational Study. Geometry optimizations and electrostatic potential calculations were performed on the uncoordinated anions, $[NbOF_5]^{2-}$ and $[WO_2F_4]^{2-}$. The geometry of $[NbOF_5]^{2-}$ and $[WO_2F_4]^{2-}$ was optimized by using symmetry constraints, C_s and C_{2v}, respectively, in GAMESS-US.[9] GAMESS-US implementation of B3LYP functional and the SBKJC ECP + valence basis set augmented by d functions was employed. A final Hessian calculation confirmed the optimized geometry to be a minimum. See Supporting Information. An electrostatic potential calculation was performed on each anion in GAMESS-US. The electrostatic potential maps shown in parts a and b of Figure 5 were created with MOLDEN.[10]

Table 2. Selected Bond Lengths (Å) for Ordered $[VOF_5]^{2-}$, $[NbOF_5]^{2-}$, and $[WO_2F_4]^{2-}$ Anions

bond	bond length (Å)	bond	bond length (Å)
		$[NbOF_5]^{2-}$	
$[pyH]_2[Cu(py)_4(NbOF_5)_2]$		$Cu(pyz)_2NbOF_5\cdot(pyz)(H_2O)$	
Nb−O(1)	1.728(8)	Nb−O(1)	1.777(5)
Nb−F(1)	1.937(6)	Nb−F(1)	1.914(4)
Nb−F(2)	1.927(5)	Nb−F(2)	1.918(4)
Nb−F(3)	2.099(8)	Nb−F(3)	2.075(4)
geometry optimized $[NbOF_5]^{2-}$		$[HNC_6H_6OH]_2[Cu(py)_4(NbOF_5)_2]$	
Nb−O(1)	1.771	Nb−O(1)	1.763(1)
Nb−F(1)	2.013	Nb−F(1)	1.936(1)
Nb−F(2)	2.013	Nb−F(2)	1.912(1)
Nb−F(3)	2.011	Nb−F(3)	1.924(1)
Nb−F(4)	2.011	Nb−F(4)	1.981(1)
Nb−F(5)	2.129	Nb−F(5)	2.098(1)
		$[WO_2F_4]^{2-}$	
$Na_2WO_2F_4$		$[HNC_6H_6OH]_2[Cu(py)_4(WO_2F_4)_2]$	
W−O	1.750(9)	W−O(1)	1.772(2)
W−F(1)	1.932(9)	W−O(2)	1.714(2)
W−F(2)	2.039(9)	W−F(1)	2.059(2)
		W−F(2)	2.029(2)
geometry optimized $[WO_2F_4]^{2-}$		W−F(3)	1.903(2)
W−O	1.755	W−F(4)	1.908(2)
W−F(1)	1.987		
W−F(2)	2.085		
		$[VOF_5]^{2-}$	
$[pyH]_2[Cu(py)_4(VOF_5)_2]$			
V−O(1)	1.596(2)		
V−F(1)	2.084(2)		
V−F(2)	1.819(2)		
V−F(3)	1.883(2)		
V−F(4)	1.811(2)		
V−F(5)	1.836(2)		

Results

The $[NbOF_5]^{2-}$ anion in $[HNC_6H_6OH]_2[Cu(py)_4(NbOF_5)_2]$ consists of a central Nb^{5+} cation bound to an oxide and five fluoride ligands. The IR band at 905 cm^{-1}, indicative of an Nb−O stretch, confirms the presence of the $[NbOF_5]^{2-}$ anion. The Nb−O(1) bond is short, 1.763(1) Å, resulting in a long bond to the trans fluoride F(5), 2.098(1) Å. The four equatorial fluoride Nb−F distances range from 1.912(1) to 1.981(1) Å. The Jahn−Teller distortion of Cu^{2+} (d^9) is observed through two "long" Cu−O(1) bonds to the $[NbOF_5]^{2-}$ anions of 2.307(2) Å and four "short" bonds to coordinated pyridines of 2.065(2) Å, 2.038(2) Å × 2, and 2.066(2) Å. Characteristic IR bands for coordinated pyridine are present, most notably the C═C and C═N stretches at 1556 and 1623 cm^{-1} and the N−Cu stretch at 627 cm^{-1}. The result is an anionic cluster, $[Cu(py)_4(NbOF_5)_2]^{2-}$, in

(6) *TEXSAN*: *Crystal Structure Analysis Package*; Molecular Structure Corp.: The Woodlands, TX, 1985 and 1992.
(7) Sheldrick, G. M. SHELXS86. In *Crystallographic Computing 3*; Sheldrick, G. M., Kruger, C., Goddard, R., Eds.; Oxford University Press: Oxford, UK, 1985; pp 175−189.
(8) Beurskens, P. T.; Admiraal, G.; Beurskens, G.; Bosman, W. P.; de Gelder, R.; Israel, R.; Smits, J. M. M. *The DIRDIF_94 program system*; Technical Report of the Crystallographic Laboratory; University of Nijmegen: Nijmegen, The Netherlands, 1994.
(9) GAMESS: Schmidt, M. W.; Baldridge, K. K.; Boatz, J. A.; Elbert, S. T.; Gordon, M. S.; Jensen, J. H.; Koseki, S.; Matsunaga, N.; Nguyen, K. A.; Su, S. J.; Windus, T. L.; Dupuis, M.; Montgomery, J. A. *J. Comput. Chem.* **1993**, *14*, 1347−1363.
(10) Schaftenaar, G.; Noordik, J.H. MOLDEN, a pre- and post-processing program for molecular and electronic structures. *J. Comput.-Aided Mol. Design* **2000**, *14*, 123−134.

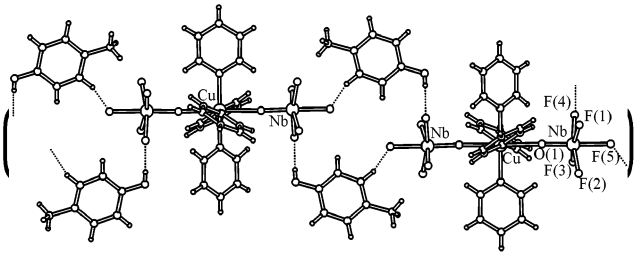

Figure 2. One-dimensional chain of $[HNC_6H_6OH]_2[Cu(py)_4(NbOF_5)_2]$ showing each $[HNC_6H_6OH]^+$ cation hydrogen bonding to two adjacent $[Cu(py)_4(NbOF_5)_2]^{2-}$ anionic clusters. Dashed lines represent hydrogen bonding interactions.

which two $[NbOF_5]^{2-}$ anions coordinate through O(1) to the central $[Cu(py)_4]^{2+}$ cation in a trans fashion.

The role of the 5-hydroxy-2-methylpyridinium cation, $[HNC_6H_6OH]^+$, is twofold. First, it balances the charge of the anionic $[Cu(py)_4(NbOF_5)_2]^{2-}$ clusters. Second, it hydrogen bonds through both the hydroxyl group and the protonated amine to adjacent $[Cu(py)_4(NbOF_5)_2]^{2-}$ clusters. As expected, because the $[NbOF_5]^{2-}$ anion is trans directing,[11] the fluoride trans to the oxide ligand, F(5), accepts a hydrogen bond from the protonated amine, H(16) bound to N(4). Completing the bond network, H(14) on the hydroxyl group hydrogen bonds to F(4), an equatorial fluoride on a second anionic cluster. Neutral one-dimensional chains form as a result of each $[HNC_6H_6OH]^+$ cation forming hydrogen bonds to two adjacent $[Cu(py)_4(NbOF_5)_2]^{2-}$ clusters. See Figures 1 and 2. These chains, which reflect the 2:1 stoichiometry of the crystal, are aligned in layers in the *ac* plane separated by van der Waals forces. See Figure 3.

Hydrogen bonding from $[HNC_6H_6OH]^+$ cations to the $[NbOF_5]^{2-}$ anions affects the Nb−F bond lengths. The Nb−F(4) bond, 1.981(1) Å, longer than the Nb−F(1), F(2) or F(3) bonds, forms a hydrogen bond with the hydroxide on 5-hydroxy-2-methylpyridinium. The Nb−F(4) bond weakens as F(4) accepts this hydrogen bond, resulting in a shorter, stronger Nb−F(2) bond, 1.912(1) Å, in the trans position. The Nb−F(1) and F(3) bonds are not affected and they exhibit intermediate bonds lengths, 1.936(1) and 1.924(1) Å, respectively.

The geometry optimization of $[NbOF_5]^{2-}$ reveals a short Nb−O bond, 1.771 Å, and a long bond to the trans fluoride, 2.129 Å. The four equatorial Nb−F bonds are 2 × 2.011 Å and 2 × 2.013 Å in length. Thus the anion adopts approximately C_{4v} symmetry. The ionic charges on the niobium, oxide, and fluorides were calculated by using Mulliken populations, Lowdin populations, and natural bond order (NBO) analysis and are listed in Table 3. The total molecular charge was constrained to be −2, which is reflected in the sum of ionic charges. From the natural localized molecular orbital (NLMO) calculations, the orbitals involved in bonding between the oxide and the niobium are, as expected, the Nb 4d and 5s orbitals and the oxide 2s and 2p orbitals.[12,13] Bonding between the niobium and fluorides occurs from overlap between the Nb 4d and 5s orbitals and the fluoride 2s and

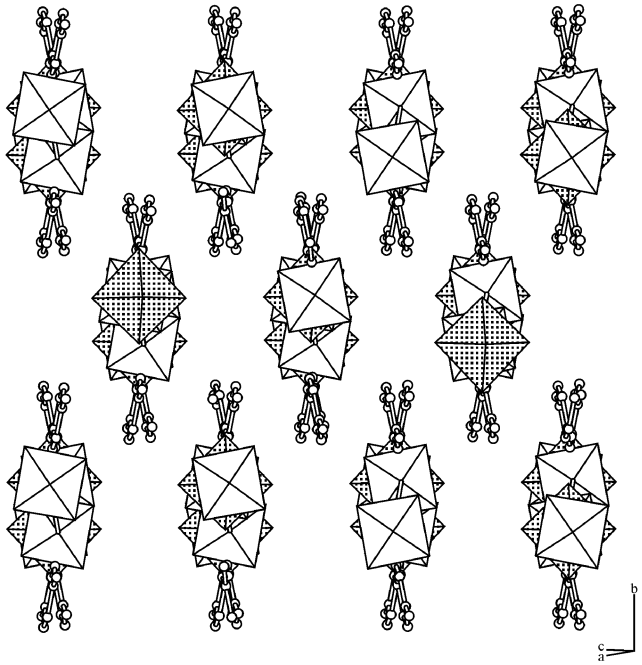

Figure 3. Three-dimensional packing of $[HNC_6H_6OH]_2[Cu(py)_4(NbOF_5)_2]$. Shaded and unshaded octahedra represent $[Cu(py)_4]^{2+}$ and $[NbOF_5]^{2-}$, respectively. Coordinated pyridine rings and hydrogen atoms have been removed for clarity.

Table 3. Mulliken, Lowdin, and Natural Bond Order Ionic Charges (in electrons)

atom	Mulliken	Lowdin	NBO
		$[NbOF_5]^{2-}$	
Nb	2.134163	1.645406	2.30734
O	−0.491363	−0.634053	−0.84702
F(1)	−0.692155	−0.584868	−0.67390
F(2)	−0.691881	−0.584799	−0.67384
F(3)	−0.695086	−0.586173	−0.67503
F(4)	−0.695086	−0.586173	−0.67503
F(5)	−0.868592	−0.669341	−0.76252
total	−2.000000	−2.000000	−2.00000
		$[WO_2F_4]^{2-}$	
W	1.428632	1.716627	2.66743
O(1)	−0.498070	−0.647525	−0.88965
O(2)	−0.498070	−0.647525	−0.88965
F(1)	−0.645384	−0.630545	−0.75521
F(2)	−0.645384	−0.630545	−0.75521
F(3)	−0.570862	−0.580244	−0.68885
F(4)	−0.570862	−0.580244	−0.68885
total	−2.000000	−2.000000	−2.00000

2p orbitals. The most reactive region around the $[NbOF_5]^{2-}$ anion is near the trans fluoride as shown by the red and yellow colors in the electrostatic potential map. See Figure 5a. This is in good agreement with bond valence sums on previously studied compounds containing the $[NbOF_5]^{2-}$ anion.[14]

The geometry optimization of $[WO_2F_4]^{2-}$ exhibits short W−O bonds, 2 × 1.755 Å, and long bonds to the trans fluorides, 2 × 2.085 Å, while the two cis W−F bonds are 2

(11) Halasyamani, P. S.; Willis, M. J.; Stern, C. L.; Lundquist, P. M.; Wong, G. K.; Poeppelmeier, K. R. *Inorg. Chem.* **1996**, *35*, 1367.

(12) Glendening, E. D.; Badenhoop, J. K.; Reed, A. E.; Carpenter, J. E.; Weinhold, F. *NBO 4.M*; Theoretical Chemistry Institute, University of Wisconsin: Madison, WI, 1999.

(13) Reed, A. E.; Weinhold, F. *J. Chem. Phys.* **1985**, *83*, 1736.

(14) Heier, K. R.; Norquist, A. J.; Wilson, C. G.; Stern, C. L.; Poeppelmeier, K. R. *Inorg. Chem.* **1998**, *37*, 76.

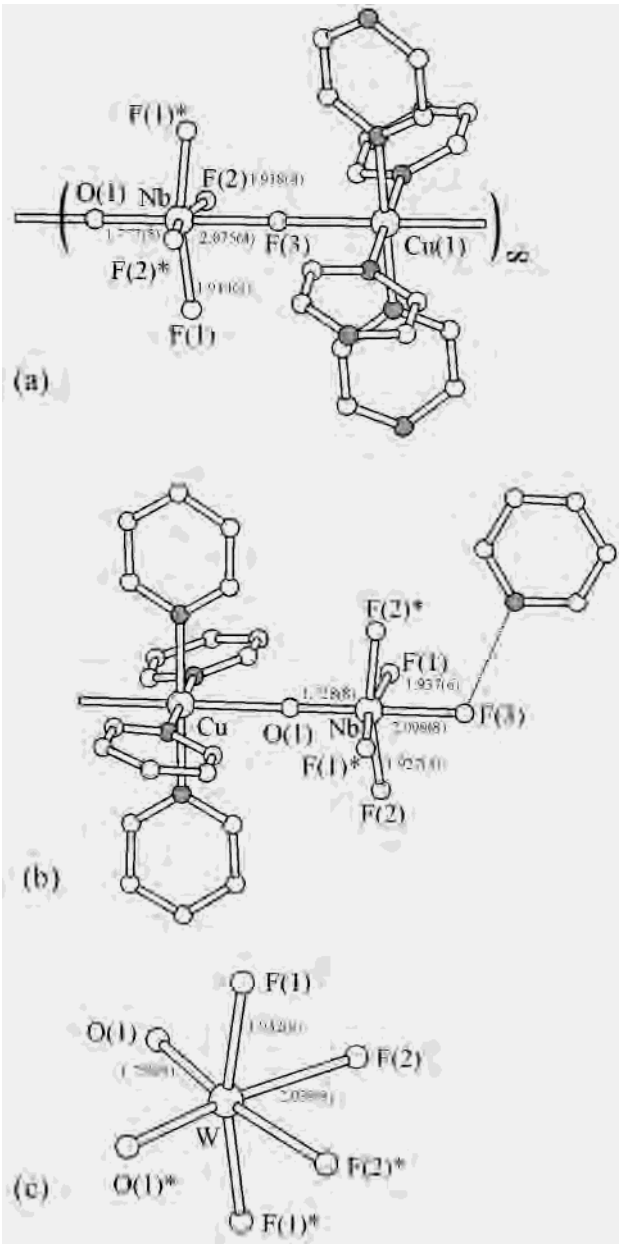

Figure 4. Primary distortions in (a) $Cu(pyz)_2NbOF_5 \cdot (pyz)(H_2O)$, (b) $[pyH]_2[Cu(py)_4(NbOF_5)_2]$, and (c) the $[WO_2F_4]^{2-}$ anion in $Na_2WO_2F_4$. Selected bond lengths are included (Å). Dashed line denotes hydrogen-bonding interactions. Hydrogen atoms have been removed for clarity. Shaded atoms represent nitrogen atoms.

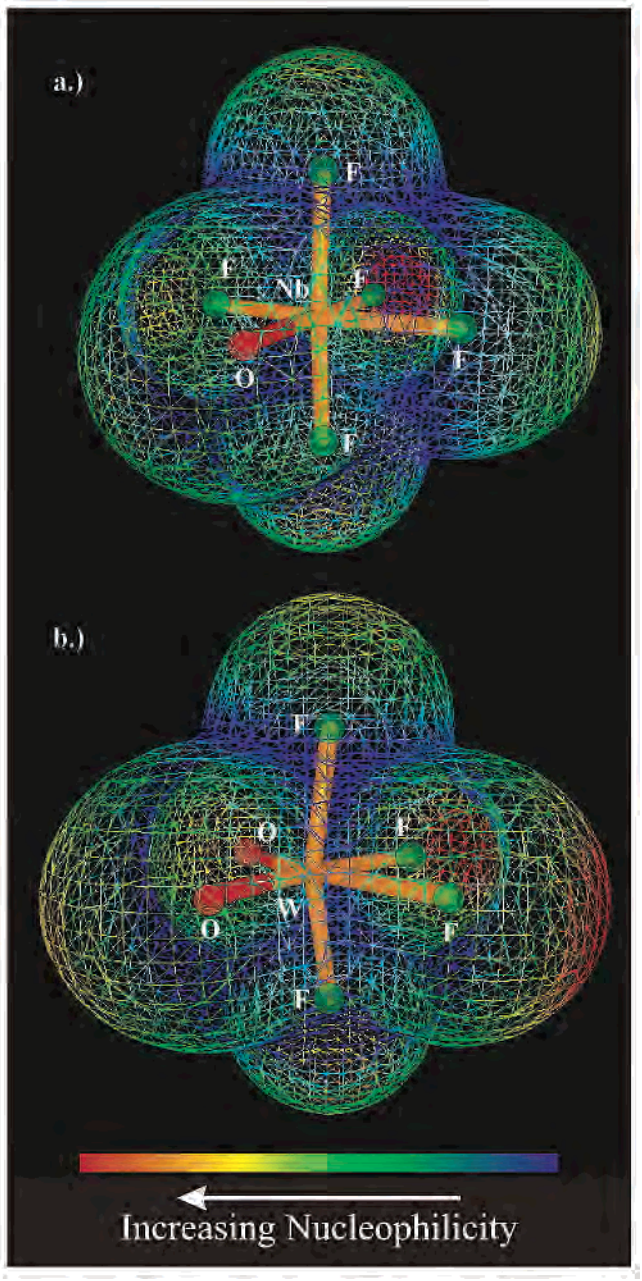

Figure 5. Geometry optimized (a) $[NbOF_5]^{2-}$ and (b) $[WO_2F_4]^{2-}$ anions with a spherical grid showing the electrostatic potential around the anion. Red denotes the most reactive potential areas, while blue denotes the least reactive potential areas.

× 1.987 Å in length. The ionic charges on the tungsten, oxide, and fluorides were calculated by using Mulliken populations, Lowdin populations, and natural bond order (NBO) analysis. See Table 3. The total molecular charge was constrained to be −2. From the NLMO calculations, the orbitals involved in bonding between the oxide and the tungsten are the W 5d and 6s orbitals and the oxide 2s and 2p orbitals.[12,13] Bonding between the tungsten and fluorides occurs from overlap between the W 5d and 6s orbitals and the fluoride 2s and 2p orbitals. The electrostatic potential map around the $[WO_2F_4]^{2-}$ anion shows significant reactivity near all the ligands. See Figure 5b. The reactivity is somewhat greater near the oxides and trans fluorides, in agreement with bond valence sums on previously studied compounds containing the $[WO_2F_4]^{2-}$ anion.[15,16]

Discussion

Of the four factors that play a role in the occurrence of out-of-center distortions—electronic effects, bond networks, lattice stresses, and cation−cation repulsions—the first two factors are responsible for distortions in early transition metal oxide fluoride anions of the formula $[MO_xF_{6-x}]^{2-}$ ($x = 1$, M

(15) Chaminade, J. P.; Moutou, J. M.; Villeneuve, G.; Couzi, M.; Pouchard, M.; Hagenmuller, P. *J. Solid State Chem.* **1986**, *65*, 27.
(16) Welk, M. E.; Norquist, A. J.; Stern, C. L.; Poeppelmeier, K. R. *Inorg. Chem.* **2001**, *40*, 5479.

= V, Nb, Ta; and $x = 2$, M = Mo, W). Electronic effects are responsible for the short M−O bonds; weaker interactions between the oxide fluoride anion and the extended structure modify the coordination environment of d^0 cations. Lattice stresses, when bonds are stretched or compressed from their ideal bond lengths to conform in three dimensions, are not present as the oxide and fluoride ligands in the following reported compounds have appropriate M−O/F bond lengths.[4] See Table 2. The intrachain or intracluster distances between transition metal cations are approximately 4 Å and the cations are separated (screened) by an oxide or fluoride ion, thus no significant cation−cation repulsions are present. Six examples are described, three to illustrate electronic effects and three to show the effect the bond network has on the structure of the oxide fluoride anion.

Electronic Effects. Second-order Jahn−Teller character[17−21] arises from mixing between vacant d orbitals of the cation and filled p orbitals of the ligands. This occurs when the energy of the d orbitals has been sufficiently lowered as the cation becomes smaller and more highly charged. The degeneracy of the electronic configurations can be removed by spontaneous distortion. The occurrence, magnitude, and direction of such a distortion in a mixed metal oxide are dependent on the extended structure of the crystal.[4] However, in the $[MO_xF_{6-x}]^{2-}$ anions, only the filled p orbitals of the oxide ligands mix with vacant cation d orbitals because the energy of the fluoride p orbitals is too low for any significant mixing to occur. The result is a spontaneous distortion of the central cation toward each oxide ligand. The primary distortion can be to a corner, edge, or face of the octahedron, depending on the number of oxide ligands (one, two, or three).[22] The out-of-center distortion is inherent to the $[MO_xF_{6-x}]^{2-}$ anion and is not dependent on the extended crystal structure. This is demonstrated in this work by density functional theory calculations. Further evidence is the observation of short, strong metal−oxide bonds with use of infrared spectroscopy in compounds in which the oxide fluoride anion is disordered.[23,24]

The three-dimensional structures of $Cu(pyz)_2NbOF_5 \cdot (pyz)(H_2O)$ (pyz = $N_2C_4H_4$),[25] $[pyH]_2[Cu(py)_4(NbOF_5)_2]$,[11] and $Na_2WO_2F_4$)[15] are quite varied. $Cu(pyz)_2NbOF_5 \cdot (pyz)(H_2O)$ is a three-dimensional neutral framework material, $[pyH]_2[Cu(py)_4(NbOF_5)_2]$ contains zero-dimensional anionic clusters, and $Na_2WO_2F_4$ is comprised of $[WO_2F_4]^{2-}$ anions and Na^+ cations. Despite these differences, each structure contains crystallographically ordered oxide fluoride anions in which only a primary distortion is observed. See Figure 4. The approximate point symmetry identified in the three examples that follow is not the crystallographic site symmetry, but the approximate symmetry of the anion as it appears within the structure.

$Cu(pyz)_2NbOF_5 \cdot (pyz)(H_2O)$ consists of one-dimensional chains of alternating $[Cu(pyz)_{4/2}]^{2+}$ cations and $[NbOF_5]^{2-}$ anions linked through pyrazine spacers. See Figure 4a. The bonding interactions which could cause "secondary" distortions are Cu(1)−F(3) and Cu(2)−O(1). However, the primary distortion shares the O(1)−Nb−F(3) bond axis with these two interactions. The result is an anion in which the four equatorial Nb−F bonds are of similar lengths (within error) and the anion has an approximate point symmetry of C_{4v}.

The chemically inequivalent bond network contacts around the $[NbOF_5]^{2-}$ anion in $[pyH]_2[Cu(py)_4(NbOF_5)_2]$ interact at identical positions as in $Cu(pyz)_2NbOF_5 \cdot (pyz)(H_2O)$. $[pyH]_2[Cu(py)_4(NbOF_5)_2]$ consists of anionic $[Cu(py)_4(NbOF_5)_2]^{2-}$ clusters to which $[pyH]^+$ cations are hydrogen bound. See Figure 4b. Each anion is covalently bound to a Cu^{2+} cation through O(1) and accepts a hydrogen bond from $[pyH]^+$ through F(3). These two different coordinating groups again share the bond axis of the primary distortion, O(1)−Nb−F(3), thus no secondary distortion is observed. The approximate point symmetry of the anion remains high, C_{4v}.

The solid-state structure of $Na_2WO_2F_4$ is quite different from either $Cu(pyz)_2NbOF_5 \cdot (pyz)(H_2O)$ or $[pyH]_2[Cu(py)_4(NbOF_5)_2]$, yet it shares the common feature of a primary distortion. See Figure 4c. The $[WO_2F_4]^{2-}$ anions pack among the smaller Na^+ cations. Individual oxide or fluoride ligands have two Na^+ nearest neighbors, each at either a long (2.44 Å) or a short (2.26 Å) distance. All three possible coordination combinations exist: two long interactions, one long and one short interaction, and two short interactions. These six coordination sites (two of each possible combination) are symmetrically arranged about the $[WO_2F_4]^{2-}$ anion. Both oxide ligands are coordinated by two long interactions: the trans fluorides, F(2), are coordinated by two short interactions; the cis fluorides, F(1), are coordinated by a long and a short interaction. Despite every ligand interacting with the bond network, no secondary distortion develops owing to the symmetrical contacts, only a primary distortion. The approximate point symmetry of the anion is C_{2v}.

These experimental observations are supported by single point density functional theory (DFT) calculations that reveal the optimized geometry and the electrostatic potential around the $[NbOF_5]^{2-}$ and the $[WO_2F_4]^{2-}$ anions. See Figure 5. The geometry optimized bond lengths are close to the observed bond lengths in all three examples, differing by ±0.08 Å at most. See Table 2. The distortion present after optimization is a result of a primary distortion, as no coordinating cation was included in the calculation. The magnitude and orientation of the distortion toward the oxide ligands closely matches those in $Cu(pyz)_2NbOF_5 \cdot (pyz)(H_2O)$, $[pyH]_2[Cu(py)_4(NbOF_5)_2]$, and $Na_2WO_2F_4$ discussed above.

The Bond Network. The second cause of out-of-center distortions in d^0 transition metals, which is less obvious and more difficult to quantify, is dependent on the three-

(17) Burdett, J. K. *Molecular Shapes*; Wiley-Interscience: New York. 1980.
(18) Wheeler, R. A.; Whangbo, M. H.; Hughbanks, T.; Hoffmann, R.; Burdett, J. K.; Albright, T. A. *J. Am. Chem. Soc.* **1986**, *108*, 2222.
(19) Munowitz, M.; Jarman, R. H.; Harrison, J. F. *Chem. Mater.* **1993**, *5*, 661.
(20) Philips, M. L. F.; Harrison, W. T. A.; Gier, T. E.; Stucky, G. D.; Kulkarni, G. V.; Burdett, J. K. *Inorg. Chem.* **1990**, *29*, 2158.
(21) Kang, S. K.; Tang, H.; Albright, T. A. *J. Am. Chem. Soc.* **1993**, *115*, 1971.
(22) Goodenough, J. B. *Annu. Rev. Mater. Sci.* **1998**, *28*, 1.
(23) Heier, K. R.; Poeppelmeier, K. R. *J. Solid State Chem.* **1997**, *133*, 576.
(24) Halasyamani, P. S.; Heier, K. R.; Stern, C. L.; Poeppelmeier, K. R. *Acta. Crystallogr. Sect. C* **1997**, *53*, 1240.
(25) Halasyamani, P. S.; Heier, K. R.; Willis, M. J.; Stern, C. L.; Poeppelmeier, K. R. *Z. Anorg. Allg. Chem.* **1996**, *622*, 479.

dimensional structure. When a ligand in a $[MO_xF_{6-x}]^{2-}$ anion interacts with an nearby cation, either covalently or through a hydrogen bond, the M−O or M−F bond is weakened somewhat and its length increases. However, the oxide or fluoride ligand remains strongly bound to the positively charged central cation. The central cation then forms shorter, stronger bonds with the other ligands to maintain its atomic valence. As a result, this secondary type of distortion is smaller in magnitude than a primary distortion, and therefore only modifies the already present primary distortion in the $[MO_xF_{6-x}]^{2-}$ anions. Descriptions of three compounds, $[pyH]_2[Cu(py)_4(VOF_5)_2]$,[26] $[HNC_6H_6OH]_2[Cu(py)_4(NbOF_5)_2]$ (this work), and $[HNC_6H_6OH]_2[Cu(py)_4(WO_2F_4)_2]$,[16] follow which illustrate different circumstances that produce a detectable secondary distortion.

In $[pyH]_2[Cu(py)_4(VOF_5)_2]$, the crystallographically ordered $[VOF_5]^{2-}$ anion exhibits a secondary distortion caused by the bond network. In general, the $[VOF_5]^{2-}$ anion does not direct coordination along the primary O−V−F distortion bond axis. Instead, coordination is preferential to the fluoride trans to the oxide ligand and an equatorial fluoride, owing to a significant increase in the vanadium oxide bond valence.[26] Thus, the $[VOF_5]^{2-}$ anion is bound to the $[Cu(py)_4]^{2+}$ cation through F(3), an equatorial fluoride, and accepts a hydrogen bond through the trans fluoride F(1). See Figure 6a. As F(3) coordinates to $[Cu(py)_4]^{2+}$ as well as V^{5+}, while F(2), F(4), and F(5) only coordinate to V^{5+}, the four vanadium−equatorial fluoride bond lengths differ significantly: V−F(3) is 1.883(2) Å versus 1.836(2), 1.811(2), and 1.819(2) Å for the remaining three fluorides. This difference is a secondary distortion. The formation of a hydrogen bond with F(1) does not produce a detectable secondary distortion, because any lengthening of the V−F(1) bond is masked by the primary distortion of the vanadium toward the oxide ligand. The presence of the secondary distortion in $[pyH]_2[Cu(py)_4(VOF_5)_2]$ modifies the primary distortion and results in a drastic lowering of the approximate point symmetry of the $[VOF_5]^{2-}$ anion to C_1.

Three bonding interactions in $[HNC_6H_6OH]_2[Cu(py)_4(NbOF_5)_2]$ cause a detectable secondary distortion, compared to no secondary distortion when only two interactions are present in $[pyH]_2[Cu(py)_4(NbOF_5)_2]$. See Figures 4b and 6b. $[HNC_6H_6OH]_2[Cu(py)_4(NbOF_5)_2]$ contains a central anionic cluster, $[Cu(py)_4(NbOF_5)_2]^{2-}$, that is charge balanced by two protonated amines. Coordination to the anion occurs through three anionic ligands: O(1) coordinates to $[Cu(py)_4]^{2+}$, F(5) coordinates to the protonated amine on one $[HNC_6H_6OH]^+$ cation, and F(4) coordinates to the hydroxyl group on a second $[HNC_6H_6OH]^+$ cation. The donation of a hydrogen bond from the $[HNC_6H_6OH]^+$ hydroxyl group to the equatorial fluoride F(4) in $[HNC_6H_6OH]_2[Cu(py)_4(NbOF_5)_2]$ causes the Nb−F(4) bond to lengthen 1.981(1) Å and the trans Nb−F(2) bond to shorten 1.912(1) Å with respect to the other two equatorial Nb−F bonds, 1.936(1) and 1.924(1) Å. See Figure 6b. This secondary distortion modifies the primary distortion already present. Coordination to the oxide O(1) and the trans fluoride F(5) does not produce a secondary distortion, as already seen in $[pyH]_2[Cu(py)_4(NbOF_5)_2]$, because any changes in the Nb−O and Nb−F bond lengths are indistinguishable from the effects of the primary distortion. The approximate point symmetry of the $[NbOF_5]^{2-}$ anion is reduced to C_1.

The crystallographically ordered compound $[HNC_6H_6OH]_2[Cu(py)_4(WO_2F_4)_2]$, isostructural with $[HNC_6H_6OH]_2[Cu(py)_4(NbOF_5)_2]$, also exhibits both a primary and a secondary distortion.[16] Again, three contacts are made to the anion: O(1) coordinates to $[Cu(py)_4]^{2+}$, F(2) accepts a

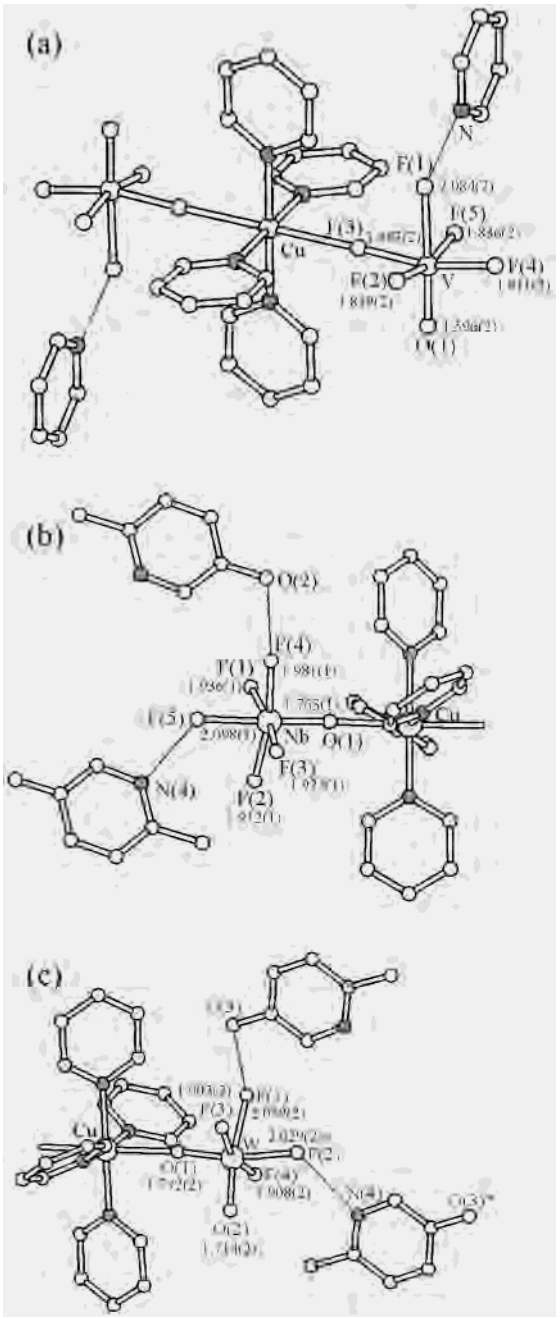

Figure 6. Primary and secondary distortions in (a) $[pyH]_2[Cu(py)_4(VOF_5)_2]$, (b) $[HNC_6H_6OH]_2[Cu(py)_4(NbOF_5)_2]$, and (c) $[HNC_6H_6OH]_2[Cu(py)_4(WO_2F_4)_2]$. Selected bond lengths are included (Å). Dashed lines denote hydrogen-bonding interactions. Hydrogen atoms have been removed for clarity. Shaded atoms represent nitrogen atoms.

(26) Welk, M. E.; Norquist, A. J.; Stern, C. L.; Poeppelmeier, K. R. *Inorg. Chem.* **2000**, *39*, 3946.

hydrogen bond from a protonated amine, and F(1) accepts a hydrogen bond from a hydroxyl group. See Figure 6c. All three contacts to the $[WO_2F_4]^{2-}$ anion introduce a secondary distortion as none of the bonding interactions occur along the primary distortion bond axis of the tungsten toward an edge of the octahedron. The fluoride ligand F(1) in $[HNC_6H_6OH]_2[Cu(py)_4(WO_2F_4)_2]$ accepts a hydrogen bond, which lengthens the W−F(2) bond and shortens the W−O(2) bond in the trans position. Coordination of the $[Cu(py)_4]^{2+}$ cation to O(1) lengthens the W−O(1) bond and since the trans fluoride F(1) accepts a hydrogen bond, the W−F(1) distance remains long. To maintain the valence of the tungsten cation, the remaining uncoordinated cis fluorides, F(3) and F(4), form short bonds, 1.903(2) and 1.908(2) Å, respectively. The difference in W−O bond lengths, 1.772(2) versus 1.714(2) Å for O(1) and O(2), respectively, clearly demonstrates the effects of hydrogen bonding on the $[WO_2F_4]^{2-}$ anion. A significant difference between the W−F(1) and W−F(2) bond lengths also is noticeable owing to different coordination environments. The approximate point symmetry of the $[WO_2F_4]^{2-}$ anion is thereby reduced to C_1.

The observation of secondary distortions in these examples depends on two conditions: First, the anion must be crystallographically ordered because only then are bond lengths and angles calculated with sufficient accuracy to expose an anionic distortion. Second, the coordination sites of the bond network cannot be symmetrically arranged about the anion. As in the case of $Na_2WO_2F_4$, a symmetrical arrangement of contacts with the bond network causes symmetrical lengthening and shortening of bonds making detection of a secondary distortion impossible. Thus, the secondary distortion can be observed if (1) the anion is crystallographically ordered and (2) the anion either does not direct coordination along the primary distortion or, if it does, the number of coordination sites is increased and are asymmetrically arranged, as illustrated by both $[HNC_6H_6OH]_2[Cu(py)_4(NbOF_5)_2]$ and $[HNC_6H_6OH]_2[Cu(py)_4(WO_2F_4)_2]$.

Conclusion

Two different types of out-of-center distortions in octahedral d^0 transition metal oxide fluoride anions have been described and explained by using the criteria proposed by Kunz and Brown.[4] Mixing between metal d and oxide p orbitals causes primary distortions that are not dependent on the extended structure within the crystal. These primary distortions are inherent to the anion as shown by DFT calculations and can be detected in crystallographically disordered anions by IR spectroscopy. In contrast to the primary distortion, secondary distortions are solely detectable when there is crystallographic order and the bond network interactions are asymmetrical. Thus, the presence of an observable secondary distortion is wholly dependent on bonding interactions between the anion and extended structure.

Acknowledgment. The authors gratefully acknowledge support from the National Science Foundation, Solid State Chemistry (Award No. DMR 9727516), and made use of the Central Facilities supported by the MRSEC program of the National Science Foundation, at the Materials Research Center of Northwestern University (Award No. DMR 0076097).

Supporting Information Available: One X-ray crystallographic information file in CIF format including crystallographic details, atomic coordinates, anisotropic thermal parameters, interatomic distances and angles; one IR spectrum of $[HNC_6H_6OH]_2[Cu(py)_4(NbOF_5)_2]$, one text document including composition space synthesis reagent ratios, two text documents including GAMESS-US input parameters, input coordinates, convergence criteria, final absolute energy, Mulliken and Lowdin orbital population, bond order and valence analysis, natural bond orbital and natural localized molecular orbital analysis, thermochemistry data at 0, 298, and 400 K, and converged atomic coordinates. This material is available free of charge via the Internet at http://pubs.acs.org.

IC025622V